


Article

A New Series of Tungstophosphoric Acid-Polymeric Matrix Catalysts: Application in the Green Synthesis of 2-Benzazepines and Analogous Rings

Edna X. Aguilera Palacios ¹, Valeria Palermo ¹ , Angel G. Sathicq ¹, Luis R. Pizzio ^{1,*} and Gustavo P. Romanelli ^{1,2,*}

¹ Centro de Investigación y Desarrollo en Ciencias Aplicadas “Dr. Jorge J. Ronco” (CINDECA-CCT La Plata-CONICET), Universidad Nacional de La Plata, La Plata B1900AJK, Argentina

² CISA, Cátedra de Química Orgánica, Facultad de Ciencias Agrarias y Forestales, Universidad Nacional de La Plata, La Plata B1904AAN, Argentina

* Correspondence: lrpizzio@quimica.unlp.edu.ar (L.R.P.); gpr@quimica.unlp.edu.ar (G.P.R.)

Abstract: A new series of composite materials (PLMTPA) based on tungstophosphoric acid (TPA) included in a polymeric matrix of polyacrylamide (PLM), with a TPA:PLM ratio of 20/80, 40/60, and 60/40, were synthesized and well characterized by FT-IR, XRD, ³¹P MAS-NMR, TGA-DSC, and SEM-EDAX. Their acidic and textural properties were determined by potentiometric titration and nitrogen adsorption–desorption isotherms, respectively. Considering ³¹P MAS-NMR and FT-IR analyses, the main species present in the samples is the [PW₁₂O₄₀]^{3−} anion that, according to XRD results, is highly dispersed in the polymeric matrix or appears as a noncrystalline phase. The thermogravimetric analysis revealed that PLMTPA materials did not undergo any remarkable chemical changes up to 200 °C. Additionally, the PLMTPA materials showed strong acid sites whose number increased with the increment of their TPA content. Finally, PLMTPA materials were used as efficient and recyclable noncorrosive catalysts for the synthesis of 2-benzazepines and related compounds. Good yields (55–88%) and high purity were achieved by a Pictet-Spengler variant reaction between *N*-aralkylsulfonamides and *s*-trioxane in soft reaction conditions: low toluene volume, at 70 °C, for 3 h. The described protocol results in a useful and environmentally friendly alternative with operative simplicity. The best catalyst in the optimized reaction conditions, PLMTPA60/40₁₀₀, was reused six times without appreciable loss of activity.

Keywords: tungstophosphoric acid; polymeric matrix; benzo[c]azepines; heterogeneous catalysis; recyclable catalyst



Citation: Aguilera Palacios, E.X.; Palermo, V.; Sathicq, A.G.; Pizzio, L.R.; Romanelli, G.P. A New Series of Tungstophosphoric Acid-Polymeric Matrix Catalysts: Application in the Green Synthesis of 2-Benzazepines and Analogous Rings. *Catalysts* **2022**, *12*, 1155. <https://doi.org/10.3390/catal12101155>

Academic Editors: Victorio Cadierno and Raffaella Mancuso

Received: 8 September 2022

Accepted: 28 September 2022

Published: 1 October 2022

Publisher’s Note: MDPI stays neutral with regard to jurisdictional claims in published maps and institutional affiliations.



Copyright: © 2022 by the authors. Licensee MDPI, Basel, Switzerland. This article is an open access article distributed under the terms and conditions of the Creative Commons Attribution (CC BY) license (<https://creativecommons.org/licenses/by/4.0/>).

1. Introduction

The development of green chemistry has received great attention from researchers at the academic and industry levels, due to the need to preserve a global ecosystem [1,2]. In this context, the development of new materials that are environmentally friendly, robust, and have high-density active sites compared to the bulk catalyst has gained much interest in the field of suitable chemistry due to their catalytic properties in a large number of organic transformations [3–5].

In this regard, materials based on heteropolyacids, particularly those with Keggin structure, are considered greener catalysts than the corrosive liquid ones. They are safe, easy to separate, generate a low amount of waste, and present stability and high acidity. Recently, our research group reported the use of materials based on Keggin heteropolyacids in heterocycle synthesis [6], green selective oxidation [7], and biomass valorization [8].

The drawback of heteropolyacids is their low surface area (<10 m²/g), which limits their use in many transformations. This disadvantage can be overcome by dispersing

the heteropolyacids on a solid support with high surface area. Thus, the search for new materials for dispersing heteropolyacids is a pressing need [9].

Polymeric matrices are a new type of support that can be used when catalysts are employed in reactions carried out at temperatures below 200 °C, due to their relatively low thermal stability. Among them, polyvinyl alcohol–polyethyleneglycol and poly(acrylic acid-co-acrylamide) polymers were used by our group for the efficient immobilization of tungstophosphoric acid ($\text{H}_3\text{PW}_{12}\text{O}_{40}$) [10–12], its aluminum or copper salt [11,13], and polyoxotungstovanadates, such as $[\text{PVW}_{11}\text{O}_{40}]^{4-}$, $[\text{PV}_2\text{W}_{10}\text{O}_{40}]^{5-}$, $[\text{SiVW}_{11}\text{O}_{40}]^{5-}$, and $[\text{SiV}_2\text{W}_{10}\text{O}_{40}]^{6-}$ [14,15]. The hybrid materials were used as catalysts in organic reactions (anisole acylation and the selective oxidation of sulfide to sulfones) performed at low temperatures.

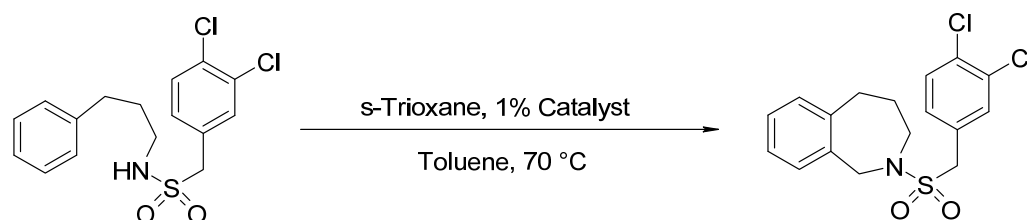
Furthermore, benzazepine derivatives are promising bioactive compounds that are generally synthesized in multiple steps, leading to the generation of stoichiometric amounts of waste [16]. They have relevant biological properties, including anxiolytic, dopaminergic, anthelmintic, antimicrobial, antitumor, anti-HIV, bronchodilator, antiarrhythmic activity, among others, and are used in Parkinson's disease treatment [17–24]. These compounds are also potentially good candidates for new drug therapies to treat skin and wounds [25]. The importance of these compounds is reflected in a very recent paper by Katalin Barta et al. In this report, the authors revealed the possibility of obtaining the benzo[c]azepine skeleton from residual biomass to be used as a platform molecule for obtaining potential bioactive molecules [26].

There are several strategies for benzo[c]azepine and analogous ring synthesis. The most suitable method to prepare these heterocycles includes the formation of the imino intermediate from arylalkylamine and a carbonyl compound, followed by an intramolecular aromatic electrophilic substitution for generating the benzazepine ring [27–29].

It is important to highlight that certain groups attached to the nitrogen atom of *N*-arylalkylamine increase the yields of the final intramolecular cyclization (an acyl or sulfonyl group notably increases the reactivity) [30].

Recently, our research group reported a suitable procedure for preparing *N*-sulfonyl-1,2,3,4-tetrahydroisoquinolines using Wells-Dawson [31] and Preyssler heteropolyacids [32] supported on silica.

In continuation of our efforts toward the development of green synthetic methodologies and a new material based on heteropolyacids, herein we report the synthesis and characterization of very efficient, suitable, and recyclable materials based on tungstophosphoric acid included in a polymeric matrix of polyacrylamide and their use as heterogeneous catalysts for the synthesis of benzo[c]azepines and analogous rings. Scheme 1 shows the synthesis of one *N*-aralkylsulfonyl-2,3,4,5-tetrahydro-1H-benzo[c]azepine using this catalytic methodology.



Scheme 1. Catalytic test for *N*-(3,4-dichlorobenzylsulfonyl)-2,3,4,5-tetrahydro-1H-benzo[c]azepine synthesis.

2. Results and Discussion

2.1. Catalyst Characterization

The polymeric matrix has $-\text{CONH}_2$ groups that can be protonated in the presence of a strong acid such as tungstophosphoric acid, allowing the electrostatic interaction of these groups and the anions $[\text{H}_{3-x}\text{PW}_{12}\text{O}_{40}]^{x-}$ (where $1 < x \leq 3$). It has been reported that H^+ transfer from $[\text{H}_3\text{PW}_{12}\text{O}_{40}]$ to the amine group, resulting in an electrostatic bond

between -NH_3^+ and $[\text{H}_{3-x}\text{PW}_{12}\text{O}_{40}]^{x-}$, is responsible for the efficient immobilization of the heteropolyanion [33,34].

The absence of W in the water solution C (obtained from the chloride elimination step) shows that TPA leaching is negligible due to the aforementioned strong interaction.

According to SEM micrographs (Figure 1), PLMTPAXX/YY samples present a sponge-like structure formed by a network of cross-linked channels. The tungsten microanalysis performed by EDAX showed that TPA content along the diameter of the spheres is almost uniform, with a slight increase on their surface.

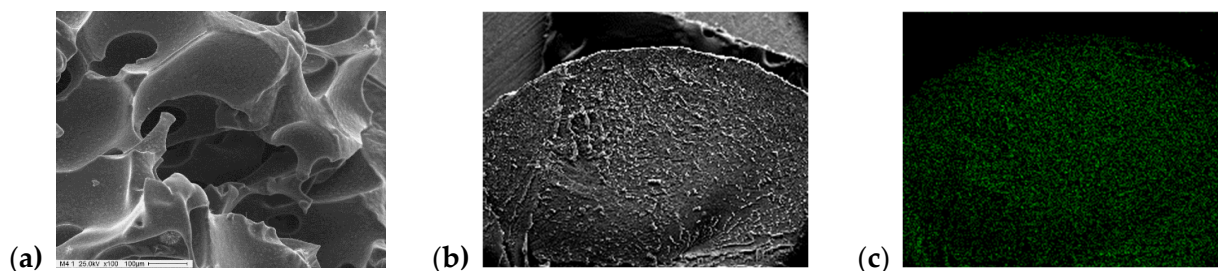


Figure 1. SEM micrograph (with (a) 100 \times and (b) 10 \times magnification) and (c) EDAX (W L α 1 line 8.396 KeV) mapping of the PLMTPA60/40 $_{\text{T100}}$ sample.

The S_{BET} values of the PLMTPA60/40 $_{\text{T100}}$, PLMTPA40/60 $_{\text{T100}}$, and PLMTPA20/80 $_{\text{T100}}$ materials are lower than 10 m^2/g (6, 4 and 3 m^2/g , respectively) and in the same range as those of the bulk TPA and PLM (9 and 2 m^2/g , respectively).

TPA FT-IR spectrum (Figure 2) shows the bands assigned to the stretching vibrations P-O $_a$ (1081 cm^{-1}), W-O $_d$ (982 cm^{-1}), W-O $_c$ -W (888 cm^{-1}), W-O $_c$ -W (793 cm^{-1}), and to the bending vibration O $_a$ -P-O $_a$ (595 cm^{-1}) [35] (see the subscript meaning in supplementary materials).

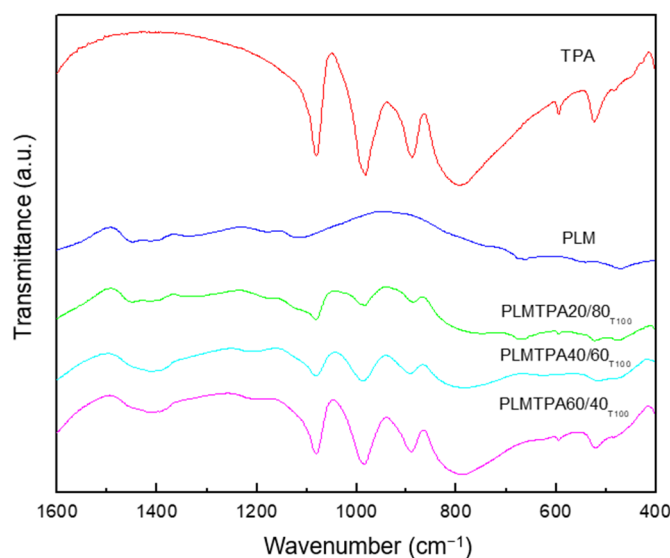


Figure 2. FT-IR spectra of PLMTPA60/40 $_{\text{T100}}$, PLMTPA40/60 $_{\text{T100}}$, and PLMTPA20/80 $_{\text{T100}}$ samples, bulk TPA and PLM.

The bands assigned to the stretching vibrations W-O $_c$ -W, W-O $_b$ -W, and P-O $_a$ in the spectrum of PLMTPA60/40 $_{\text{T100}}$, PLMTPA40/60 $_{\text{T100}}$, and PLMTPA20/80 $_{\text{T100}}$ samples overlap the characteristic bands of PLM (Figure 2). Their intensity increases with the increment of the sample TPA content, and it confirms the presence of $[\text{PW}_{12}\text{O}_{40}]^{3-}$ anion as the main species. The FT-IR spectra of samples treated at 200 and 300 $^{\circ}\text{C}$ display similar characteristics. However, in the samples calcined at a higher temperature, the relative intensity of

the TPA main bands slightly increases due to PLM chemical transformation and partial decomposition (Figure S2).

The ^{31}P MAS-NMR spectra of PLMTPA20/80_{T100}, PLMTPA40/60_{T100} and PLMTPA60/40_{T100} samples (Figure 3) display a narrow band with a maximum at around -15.0 ppm, attributed to the $[\text{PW}_{12}\text{O}_{40}]^{3-}$ anion. The PLMTPA20/80 spectrum also shows a wider and less intense band at -12.1 ppm, assigned to the $[\text{P}_2\text{W}_{21}\text{O}_{71}]^{6-}$ dimeric species [36,37].

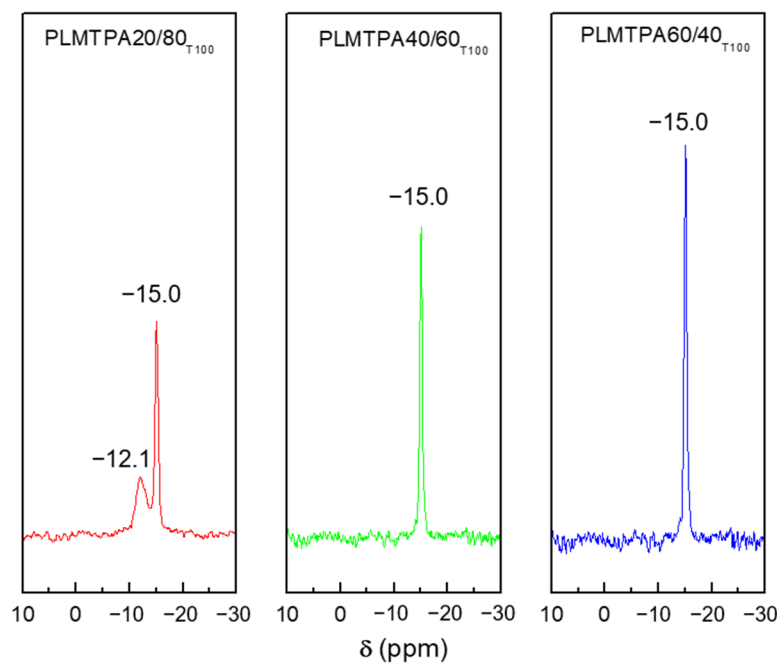


Figure 3. ^{31}P MAS-NMR spectra of PLMTPA20/80_{T100}, PLMTPA40/60_{T100} and PLMTPA60/40_{T100} samples.

Based on the FT-IR and ^{31}P MAS-NMR results, we can conclude that the $[\text{PW}_{12}\text{O}_{40}]^{3-}$ anion is the main species in the PLMTPA samples. However, the anion was partially transformed into $[\text{P}_2\text{W}_{21}\text{O}_{71}]^{6-}$ dimeric species during the synthesis due to the limited stability range of the $[\text{PW}_{12}\text{O}_{40}]^{3-}$ anion in solution [38]. No significant changes in the ^{31}P MAS-NMR spectra of the samples treated at 200 and 300 °C were found. These results agree with reports showing that an appreciable transformation of $[\text{PW}_{12}\text{O}_{40}]^{3-}$ into $[\text{P}_2\text{W}_{21}\text{O}_{71}]^{6-}$ takes place at 400 °C or higher temperatures [39].

The DSC diagram of dried PLM (Figure 4) exhibits three endothermic peaks at 199, 300 and 400 °C, which are assigned to the glass transition (T_g) and polymer decomposition [40,41]. Above T_g and up to 350 °C, the intra- and intermolecular imidization of the amido groups (with the release of NH_3) and the formation of nitrile groups from the amido group dehydration take place. At temperatures above 350 °C, imide decomposition (with the release of CO_2 and H_2O) and the rupture of the polymeric chain (with the formation of long hydrocarbon chains) occur. According to the TGA analysis, the PLM degradation takes place in two steps between 250 and 350 °C and 350 and 460 °C. The weight loss associated with these steps was 22% and 64%, respectively. TGA diagrams of PLMTPA20/80_{T100}, PLMTPA40/60_{T100} and PLMTPA60/40_{T100} samples exhibit the two aforementioned degradation steps. The weight loss ascribed to these steps decreases in parallel with the increment of TPA content in the materials (see Table S1 in supplementary materials).

The DSC diagrams of the PLMTPA20/80_{T100} and PLMTPA40/60_{T100} samples (Figure 4) present the three endothermic peaks mentioned above at slightly lower temperatures. In the case of the PLMTPA40/60_{T100} material, the peak assigned to the glass transition is barely visible. For the PLMTPA60/40_{T100} samples, the glass transition peak is not present, and the other two endothermic peaks appear at lower temperatures (279 and 385 °C). These

results show that PLMTPAXX/YY_{T100} materials do not undergo any remarkable chemical changes up to 200 °C.

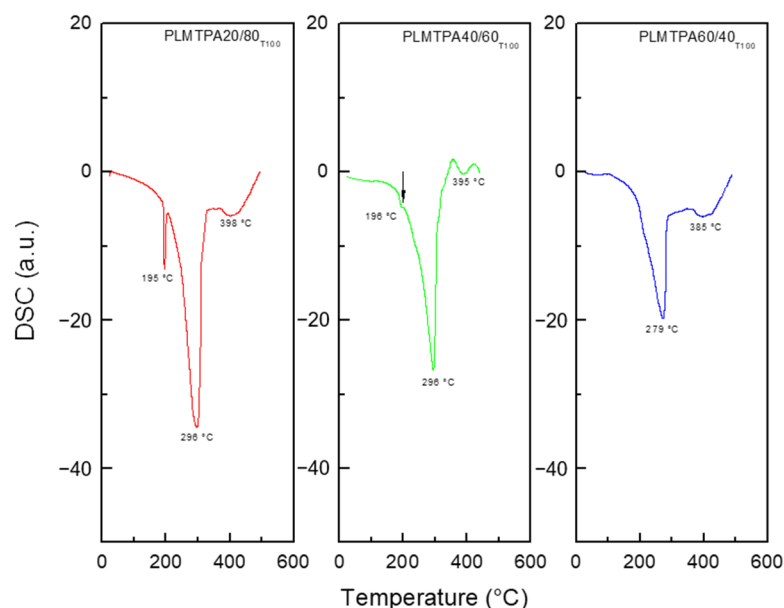


Figure 4. DSC diagrams of PLMTPA20/80_{T100}, PLMTPA40/60_{T100} and PLMTPA60/40_{T100} samples.

The XRD diagrams of the PLMTPA20/80_{T100}, PLMTPA40/60_{T100} and PLMTPA60/40_{T100} samples (Figure 5) show a new set of broad- and low-intensity peaks overlapping the XRD pattern of bulk PLM; however, they resemble neither those of the H₃PW₁₂O₄₀ (JCPDS No. 50-0657) nor those of its more common hydrates (H₃PW₁₂O₄₀·6H₂O and H₃PW₁₂O₄₀·23H₂O) [42]. The intensity of these peaks slightly increases as the TPA content rises. These results suggest that most of the TPA is present in the polymeric matrix as a noncrystalline phase. On the other hand, the small TPA crystals seem to be strongly immobilized in the PLM matrix, since they were not removed during the washing with water (three times for 24 h each) performed to eliminate the chloride. The XRD diagrams of samples treated at higher temperatures present similar characteristics.

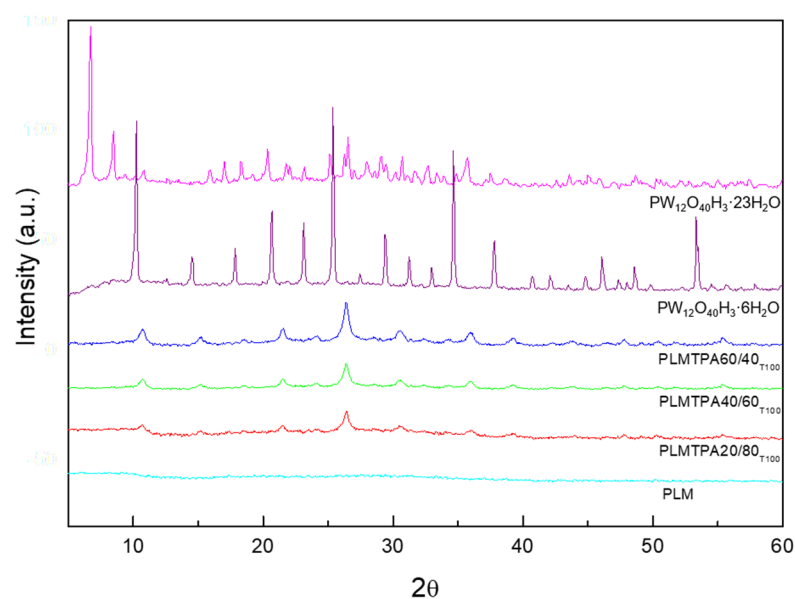


Figure 5. XRD patterns of H₃PW₁₂O₄₀·23H₂O (JCPDS No 50-0655), H₃PW₁₂O₄₀·6H₂O (JCPDS No. 50-0304), PLMTPA60/40_{T100}, PLMTPA40/60_{T100}, PLMTPA20/80_{T100}, and PLM samples.

The acidity properties of the PLMTPAXX/YY materials, estimated from the potentiometric titration with *n*-butylamine curves (Figure 6), are listed in Table 1. According to the potentiometric results, all the materials exhibit *E_i* values higher than 100 mV [43], assigned to the presence of very strong acid sites (see the classification scale in supplementary materials).

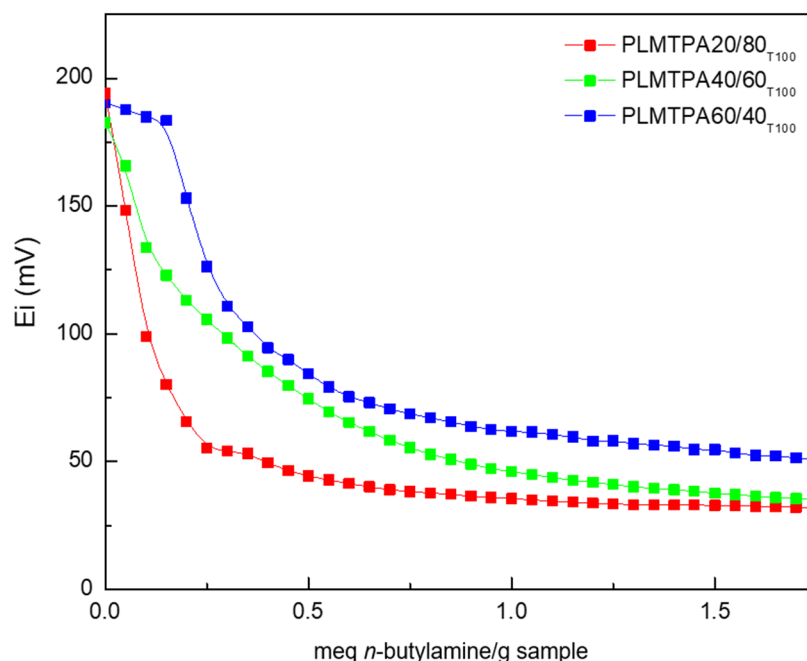


Figure 6. Potentiometric titration curves of PLMTPA20/80_{T100}, PLMTPA40/60_{T100} and PLMTPA60/40_{T100} samples.

Table 1. Effect of different catalysts on *N*-(3,4-dichlorobenzylsulfonyl)-2,3,4,5-tetrahydro-1*H*-benzo[*c*]azepine yields (%).

Entry	Catalyst	E _i (mV)	N _s ^a	Yields (%) ^b
1	None	-	-	-
2	PLM	44	-	-
3	PLMTPA20/80 _{T100}	194	84	48
4	PLMTPA40/60 _{T100}	182	146	62
5	PLMTPA60/40 _{T100}	191	201	83
6	PLMTPA60/40 _{T200}	180	158	62
7	PLMTPA60/40 _{T300}	90	77	9

Reaction conditions: *N*-phenylpropyl-3,4-dichlorobenzylsulfonamide, 0.5 mmol; *s*-trioxane, 1.5 mmol; toluene, 2 mL; catalyst, 1% mmol; 70 °C; 3 h; stirring. ^a meq/g. ^b Pure product.

The acid strength of PLMTPA20/80_{T100} (*E_i* = 194 mV), PLMTPA40/60_{T100} (*E_i* = 182 mV), and PLMTPA60/40_{T100} (*E_i* = 191 mV) samples is higher than that of PLM (*E_i* = −44 mV) but lower than that of bulk TPA (*E_i* = 620 mV) [44]. The lower acid strength of the PLMTPAXX/YY materials compared to bulk TPA could be due to the fact that the protons in TPA are present as H⁺(H₂O)₂ species (hydrated protons), whereas in the PLMTPA samples they interact with the nitrogen of -CONH₂ groups.

The number of acid sites (N_s) estimated as the area under the curve increases in the following order: PLMTPA20/80_{T100} > PLMTPA40/60_{T100} > PLMTPA60/40_{T100} (84, 146, and 201 meq *n*-butylamine/g, respectively) in parallel with the increment of TPA content. On the other hand, the thermal treatment of the samples at higher temperatures decreased

both Ei and Ns (Figure S3), because of the structural and chemical modification of the PLM matrix.

2.2. Catalytic Test for *N*-(3,4-Dichlorobenzylsulfonyl)-2,3,4,5-Tetrahydro-1*H*-Benzo[*c*]azepine Synthesis

The most suitable catalyst was identified using the test reaction between *N*-phenylpropyl-3,4-dichlorobenzylsulfonamide and *s*-trioxane as substrate (see Scheme 1), with toluene as solvent, at 70 °C for 3 h to obtain *N*-(3,4-dichlorobenzylsulfonyl)-2,3,4,5-tetrahydro-1*H*-benzo[*c*]azepine.

First, we performed a blank experiment without the catalyst, and no reaction was observed (Table 1, entry 1). Likewise, no reaction was observed when the support (PLM) was used, under the same conditions (Table 1, entry 2). Subsequently, the PLMTPA materials were tested, showing very good conversion and selectivity of the desired product (Table 1, entries 3–5). In these three experiments, very good product yields were obtained for PLMTPA20/80_{T100}, PLMTPA40/60_{T100} and PLMTPA60/40_{T100} samples (48%, 62% and 83%, respectively), indicating the need to use a catalyst with acidic properties to produce *N*-(3,4-dichlorobenzylsulfonyl)-2,3,4,5-tetrahydro-1*H*-benzo[*c*]azepine. According to the acidity measurements of the PLMTPA samples obtained by potentiometric titration, the Ns in the catalysts increases as follows: PLMTPA20/80_{T100} < PLMTPA40/60_{T100} < PLMTPA60/40_{T100}. The *N*-(3,4-dichlorobenzylsulfonyl)-2,3,4,5-tetrahydro-1*H*-benzo[*c*]azepine yield increases in the same way, suggesting that the acidity strongly affects the catalytic activity of the PLMTPA catalysts. The yields obtained for the samples calcined at 200 and 300 °C (Table 1, entries 6 and 7) confirm that the drop in Ns and acid strength leads to a decrease in *N*-(3,4-dichlorobenzylsulfonyl)-2,3,4,5-tetrahydro-1*H*-benzo[*c*]azepine production. On the other hand, the yield obtained using bulk TPA in the same reaction conditions was lower (41%) than those achieved using the PLMTPA20/80_{T100}, PLMTPA40/60_{T100}, and PLMTPA60/40_{T100} catalysts. Consequently, the TPA inclusion in the polymer matrix (mainly present as a noncrystalline phase) increases the *N*-(3,4-dichlorobenzylsulfonyl)-2,3,4,5-tetrahydro-1*H*-benzo[*c*]azepine yields and facilitates the catalyst recovery (by simple centrifugation and filtration) from the reaction medium for its subsequent reuse. On the contrary, the recovery of bulk TPA was more difficult, because it must be washed several times with the reaction solvent to eliminate product traces covering its surface.

To evaluate the influence of the solvent nature, the reaction was conducted using benzene, chloroform, dichloromethane, and hexane instead of toluene (Table 2). All solvents were selected due to TPA insolubility in them.

Table 2. Solvent effect on *N*-(3,4-dichlorobenzylsulfonyl)-2,3,4,5-tetrahydro-1*H*-benzo[*c*]azepine yields (%).

Entry	Solvent	Yields (%) ^a
1	Toluene	83
2	Benzene	80
3	Chloroform	68
4	Dichloromethane ^b	52
5	Hexane ^b	35 ^c

Reaction conditions: *N*-phenylpropyl-3,4-dichlorobenzylsulfonamide, 0.5 mmol; *s*-trioxane, 1.5 mmol; solvent, 2 mL; catalyst PLMTPA60/40_{T100}, 1% mmol; 70 °C; 3 h; stirring. ^a Pure product. ^b The reaction was performed at 40 °C. ^c The substrate is partially soluble in this reaction solvent.

Similar results were obtained using aromatic hydrocarbons such as toluene and benzene (Table 2, entries 1 and 2: 83% and 80%, respectively). The use of chlorinated solvents gives lower yields (Table 2, entries 3 and 4: 68% and 52%, respectively). Finally, hexane gives a poor yield (Table 2, entry 5: 35%) due to the very low solubility of the substrates in the reaction medium. Therefore, toluene was chosen as solvent for the next experiments because, although benzene gives comparable results, it is classified as a carcinogen, which increases the risk of cancer and other illnesses.

To evaluate the influence of reaction temperature, five temperatures (25, 50, 70, 90, and 110 °C) were checked in identical reaction conditions (see Table 3). No product formation was observed at room temperature (25 °C) (Table 3, entry 1). A temperature increase to 70 °C leads to higher *N*-(3,4-dichlorobenzylsulfonyl)-2,3,4,5-tetrahydro-1*H*-2-benzo[*c*]azepine yields. The maximum yield for a reaction time of 3 h at 70 °C is 83% (Table 3, entry 3). The catalytic performance in the reaction drops considerably when raising the temperature to 90 and 100 °C (Table 3, entries 4 and 5: 69% and 51%, respectively). In these cases, the formation of several secondary products, which were detected by TLC (and were not identified), was observed. Based on these results, 70 °C was the reaction temperature chosen for the next experiments.

Table 3. Temperature effect on *N*-(3,4-dichlorobenzylsulfonyl)-2,3,4,5-tetrahydro-1*H*-benzo[*c*]azepine yields (%).

Entry	Temperature (°C)	Yields (%) ^a
1	25	-
2	50	39
3	70	83
4	90	69
5	110	51

Reaction conditions: *N*-phenylpropyl-3,4-dichlorobenzylsulfonamide, 0.5 mmol; *s*-trioxane, 1.5 mmol; toluene, 2 mL; catalyst PLMTPA60/40₁₀₀, 1% mmol; 3 h; stirring. ^a Pure product.

Table 4 shows the results obtained under the already optimized reaction conditions (toluene as solvent and 70 °C temperature) as a function of time (0.5, 2, 3, 4, and 6 h). The reaction yields increased with time up to 3 h (Table 4, entry 3) and then remained at a constant value.

Table 4. Reaction time effect on *N*-(3,4-dichlorobenzylsulfonyl)-2,3,4,5-tetrahydro-1*H*-benzo[*c*]azepine yields (%).

Entry	Time (h)	Yields (%) ^a
1	0.5	17
2	1	38
3	2	77
4	3	83
5	4	82
6	6	80

Reaction conditions: *N*-phenylpropyl-3,4-dichlorobenzylsulfonamide, 0.5 mmol; *s*-trioxane, 1.5 mmol; toluene, 2 mL; catalyst = PLMTPA60/40₁₀₀, 1% mmol; 70 °C; stirring. ^a Pure product.

Table 5 displays the catalyst amount effect on the yield of *N*-(3,4-dichlorobenzylsulfonyl)-2,3,4,5-tetrahydro-1*H*-benzo[*c*]azepine. The reaction yields increased from 69% to 83% when the catalyst amount increased from 0.5% to 1% (Table 5, entries 1 and 2). There were no substantial changes by raising the catalyst amount up to 2% (Table 5, entries 3 and 4).

Table 5. Catalyst amount effect on *N*-(3,4-dichlorobenzylsulfonyl)-2,3,4,5-tetrahydro-1*H*-benzo[*c*]azepine yields (%).

Entry	Catalyst Amount (%)	Yields (%) ^a
1	0.5	69
2	1	83
3	1.5	83
4	2	82

Reaction conditions: *N*-phenylpropyl-3,4-dichlorobenzylsulfonamide, 0.5 mmol; *s*-trioxane, 1.5 mmol; toluene, 2 mL; catalyst PLMTPA60/40₁₀₀; 70 °C; 3 h; stirring. ^a Pure product.

The PLMTPA60/40₁₀₀ reuse was evaluated under optimized reaction conditions: substrate, 0.5 mmol; *s*-trioxane, 1.5 mmol; toluene, 2 mL; catalyst, 1% mmol; temperature, 70 °C, and reaction time, 3 h. After each run, the catalyst was filtered, washed with three portions of toluene, dried under vacuum at 25 °C for 24 h, and reused. Each reuse test is presented in Table 6, showing that the catalyst can be reused for six cycles without appreciable loss of its catalytic activity.

Table 6. Catalyst reuse effect on *N*-(3,4-dichlorobenzylsulfonyl)-2,3,4,5-tetrahydro-1*H*-benzo[*c*]azepine yields (%).

Entry	Cycle	Yields (%) ^a
1	1	83
2	2	81
3	3	83
4	4	82
5	5	77
6	6	79

Reaction conditions: *N*-phenylpropyl-3,4-dichlorobenzylsulfonamide, 0.5 mmol; *s*-trioxane, 1.5 mmol; toluene, 2 mL; catalyst PLMTPA60/40₁₀₀, 1% mmol; 70 °C; 3 h stirring. ^a Pure product.

The possible TPA leaching from the catalyst into the reaction media was evaluated as follows: a sample of PLMTPA60/40₁₀₀ catalyst (the one with the highest TPA content) was refluxed in toluene (3 mL) for 6 h, filtered in vacuum, and dried to constant weight. The activity of the PLMTPA60/40₁₀₀ catalyst was evaluated, being similar to that evaluated with the fresh catalyst (82%, 70 °C, 3 h). The refluxed toluene was used as solvent for attempting the *N*-(3,4-dichlorobenzylsulfonyl)-2,3,4,5-tetrahydro-1*H*-benzo[*c*]azepine synthesis without adding the catalyst. After 6 h at 70 °C, no significant amounts of the product were detected, and the substrate was recovered quantitatively from the reaction media.

Finally, another experiment consisted of withdrawing the catalyst after 1 h of reaction; the reaction was followed for two more hours, and the reaction yields were evaluated. The reaction yields at 1 and 3 h were practically the same (38% and 40%, respectively), indicating that the synthesis reaction takes place in a heterogeneous phase.

Using the best reaction conditions found for *N*-(3,4-dichlorobenzylsulfonyl)-2,3,4,5-tetrahydro-1*H*-benzo[*c*]azepine synthesis (*N*-aralkylsulfonamide, 0.5 mmol; *s*-trioxane, 1.5 mmol; toluene, 2 mL; catalyst, PLMTPA60/40₁₀₀, 1% mmol; and 70 °C, 3 h), various benzo[*c*]azepines, isoquinolines, and one benzo[*c*]azocine were prepared. The methodology is not appropriate to prepare analogous rings of five, eight, and nine members, because of the low yield. However, it is suitable for the preparation of heterocycles with six and seven members (Table 7).

Table 8 shows comparative results for the *N*-(3,4-dichlorobenzylsulfonyl)-2,3,4,5-tetrahydro-1*H*-benzo[*c*]azepine synthesis using different acid catalysts. Better results were obtained using heterogeneous catalysts based on HPAs (Table 8, entries 3–5), probably due to the milder conditions than the methanesulphonic acid/trifluoroacetic acid and methanesulphonic/acetic anhydride media (Table 8, entries 1 and 2).

2.3. Mechanism of 2,3,4,5-Tetrahydro-1*H*-benzo[*c*]azepine and Analogous Ring Synthesis

A plausible mechanism for the synthesis of 2,3,4,5-tetrahydro-1*H*-benzo[*c*]azepines and analogous rings is described. This reaction involves the formation of a benzazepine or a homolog in the nitrogen ring from a sulfonamide and formaldehyde formed in situ from *s*-trioxane. The reaction is catalyzed by a strong acid. The proposed mechanism corresponds to the reaction in which the catalyst is a supported HPA (Scheme 2).

Initially, the catalyst coordinates with an *s*-trioxane molecule forming the adduct (1), which undergoes nucleophilic attack by the sulfonamide, simultaneously with the protonation of *s*-trioxane, resulting in the alkylation of the N atom by a hydroxymethyl and the formation of an ammonium ion (2).

Table 7. Substrate effect on *N*-(aralkylsulfonyl)-2,3,4,5-tetrahydro-1*H*-benzo[*c*]azepine and analogous ring yields (%).

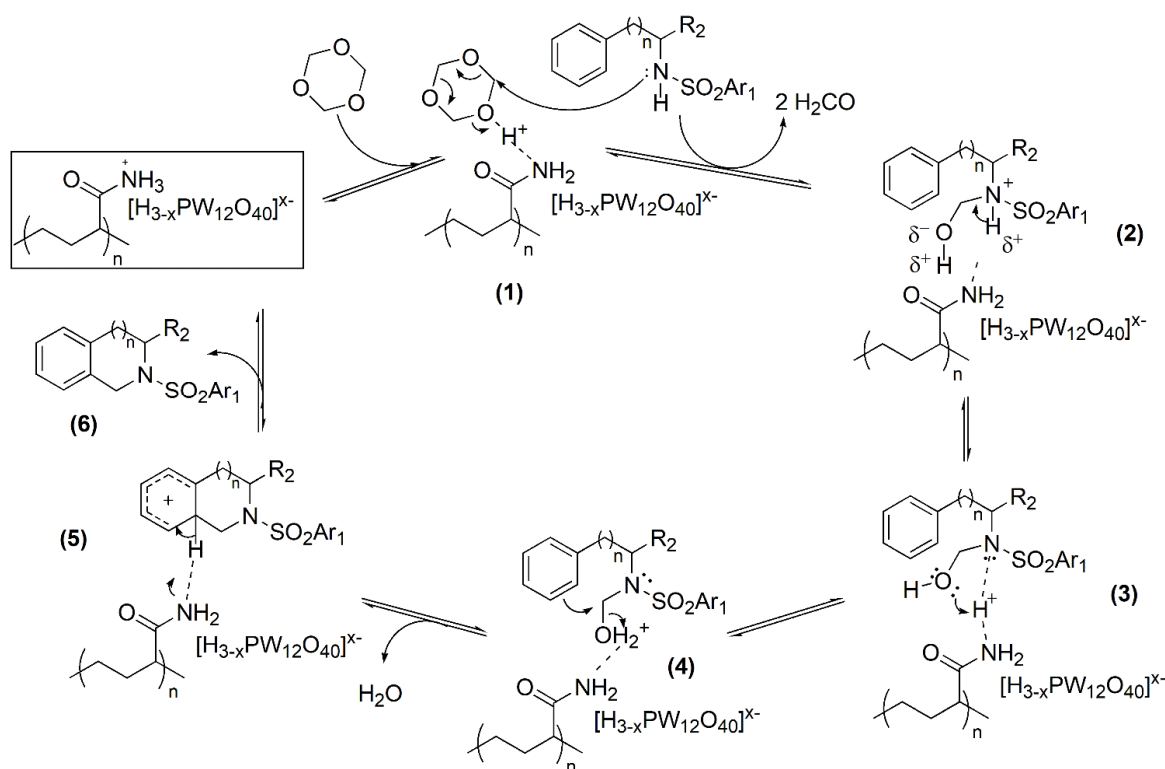
Entry	Substrate	Cycle Size	Product	Yields (%) ^a
1		6		88
2		7		83
3		6		20
4		7		-
5		7		80
6		6		55
7		6		88

Reaction conditions: *N*-aralkylsulfonamide, 0.5 mmol; *s*-trioxane, 1.5 mmol; toluene, 2 mL; catalyst PLMTPA60/40₁₀₀, 1% mmol; 70 °C; 3 h; stirring. ^a Pure product.

Table 8. Use of different catalysts on *N*-(3,4-dichlorobenzylsulfonyl)-2,3,4,5-tetrahydro-1*H*-benzo[*c*]azepine synthesis.

Entry	Catalyst	Yields (%)	Reference
1	Methanesulphonic acid/ trifluoroacetic acid	68	[30]
2	Methanesulphonic acid/ acetic anhydride	70	[30]
3	H ₆ P ₂ W ₁₈ O ₆₂ /SiO ₂	84	[31]
4	H ₁₄ [NaP ₅ W ₃₀ O ₁₁₀]/SiO ₂	81	[32]
5	PLMTPA60/40 ₁₀₀	83	This work

Data from cited references.

**Scheme 2.** Plausible mechanism for benzo[*c*]azepine and analogous ring synthesis.

At the acidic catalytic site, the conjugate base of the catalyst is generated momentarily, which stabilizes the ion by forming a bifurcated hydrogen bridge to both acidic hydrogens. A transfer of a proton protonates the catalyst again, which is coordinated to the hydroxymethylsulfonamide (3). A new proton transfer forms oxonium (4) from (3). Oxonium (4) is again coordinated with the conjugate base of the catalyst and undergoes an intramolecular electrophilic aromatic substitution while removing a molecule of water. Intermediate (5) is finally deprotonated, forming benzo[*c*]azepine (or analogous ring) (6) and regenerating the catalyst.

Since Barry Trost introduced the atom economy concept in 1991 [45] and Paul Anastas and John Warner defined the 12 principles of green chemistry [46], several groups, including ours, have started to consider the best ways to adopt this working approach. One way of verifying how close the synthesis method used is to an ideal process, from the green chemistry point of view, is using some of the green parameters defined by John Andraos and coworkers in several publications [47–49] and representing them in a polygon graphic. In our case, we decided to represent five of these parameters, atom economy (AE), reaction yield (RY), stoichiometry factor (SF), material recovery parameter (MRP), and reaction mass efficiency (RME), in a radial pentagon (Figure 7a,b). For comparative purposes, we

studied the green parameters on the same reaction with (Figure 7b) and without (Figure 7a) solvent and catalyst recovery. We noted that the change was in the MRP parameter, which increased approximately ten times when we recovered the solvent and catalyst.

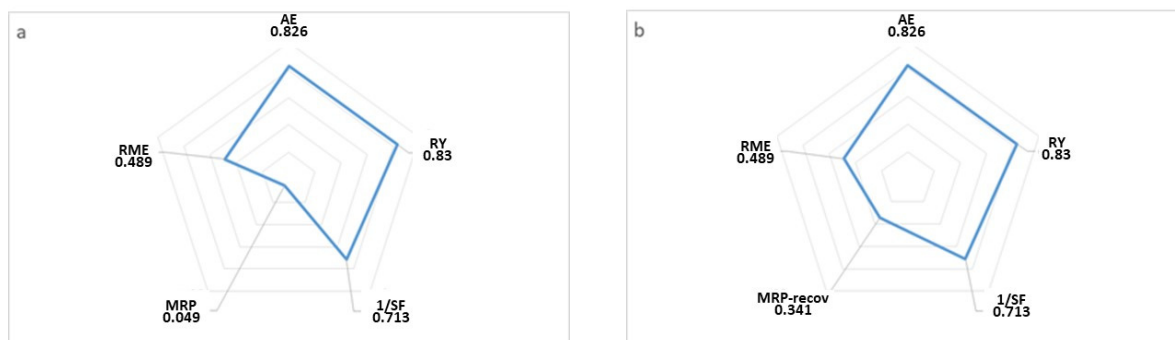


Figure 7. Radial pentagon for *N*-(3,4-dichlorobenzylsulfonyl)-2,3,4,5-tetrahydro-1*H*-benzo[*c*]azepine synthesis (a) without solvent and catalyst recovery and (b) with solvent and catalyst recovery.

3. Materials and Methods

3.1. Catalyst Preparation

First, a solution containing 7.5 g of PLM (polyacrylamide, Aldrich, Darmstadt, Germany, MW = 1.5×10^5), 180 mL of formamide (Sigma, Kawasaki, Kanagawa, Japan), and 7.5 mL of distilled water was prepared (solution A). Then, an appropriate amount of TPA ($\text{H}_3\text{PW}_{12}\text{O}_{40} \cdot 23\text{H}_2\text{O}$, Fluka, St Gallen, Switzerland dissolved in 12.5 mL of distilled water (solution B) was added to the former solution. The mixture (solution C) was stirred to homogeneity. The solution was slowly dropped into concentrated hydrochloric acid to form spherical catalyst particles. The spheres (mean diameter ~ 3 mm, see supplementary materials, Figure S1) were separated by filtration, washed (three times for 24 h each) with distilled water (until the complete elimination of Cl^-), and then dried overnight at 75°C . The amounts of TPA used were fixed to obtain a TPA:PLM ratio of 20/80, 40/60, and 60/40, respectively. Therefore, the catalysts were labeled PLMTPA20/80, PLMTPA40/60, and PLMTPA60/40. The materials were calcined at 100, 200, and 300°C for 24 h under air atmosphere. The obtained solids were named PLMTPAXX/YY100, PLMTPAXX/YY200, and PLMTPAXX/YY300, respectively. The TPA content in the PLMTPAXX/YY100 materials was estimated as the difference between the W amount in the tungstophosphoric acid water solution (solution A) and the amount of W that remained in the beaker containing the reaction mixture (solution B). Furthermore, the water samples collected from the chloride elimination step (solution C) were analyzed to evaluate the possible TPA leaching (see supplementary materials).

3.2. Sample Characterization

The nitrogen adsorption/desorption measurements were carried out at liquid nitrogen temperature (-196°C) using Micromeritics ASAP 2020 equipment (Norcross, GA, USA). From the obtained data, the specific surface area (S_{BET}) was determined using the Brunauer-Emmett-Teller model.

The morphology and structural properties of the PLMTPAXX/YY samples were characterized by scanning electron microscopy (SEM, with Philips 505 equipment, Eindhoven, Netherlands), energy-dispersive X-ray analysis (EDAX), and X-ray diffraction analysis (XRD, employing Philips PW-1732 equipment, Eindhoven, Netherlands). See more details in the supplementary materials.

The species present in the materials were evaluated by Fourier transform infrared spectroscopy (FT-IR, using Bruker IFS 66 equipment, Billerica, MA, USA) and ^{31}P nuclear magnetic resonance (P MAS-NMR, using Bruker MSL-300 equipment, Billerica, MA, USA); more details about both techniques can be found in the supplementary materials.

The acid strength and the number of acid sites were estimated from the *n*-butylamine potentiometric titration results (for more details about the technique, see supplementary materials).

TGA and DSC were carried out with Shimadzu DT 50 equipment, in an aluminum plate under nitrogen flow. The heating rate was 10 °C/min from 20 to 600 °C.

3.3. Catalytic Test for *N*-(3,4-Dichlorobenzylsulfonyl)-2,3,4,5-Tetrahydro-1*H*-Benzo[*c*]azepine Synthesis

Chemicals were purchased from Merck (Darmstadt, Germany, Aldrich, and Fluka and used after purification by standard procedures. The starting materials were prepared by procedures described in the literature. Most of the aralkylamines were obtained from the corresponding nitriles using NaBH₄-SnCl₄ [50]. The sulfonyl chlorides and the sodium sulfonates needed for their preparation were obtained by general methods [30]. The *N*-aralkylsulfonamides were prepared following Orazi et al.'s methodology [30].

The reactions were monitored by thin-layer chromatography silica gel plates coated with fluorescent indicator F254. All of the yields were calculated from pure products. Melting points were determined in sealed capillary tubes and are uncorrected. The ¹H NMR and ¹³C NMR spectra were recorded on a Bruker 400 MHz instrument as CDCl₃ solutions. All of the products were identified by a comparison of physical reported data (supplementary materials).

The PLMTPAXX/YY materials were ground (particle size, ~0.1 mm) and dried at room temperature in vacuum for 24 h. The test was performed in a reaction test tube, equipped with a reflux condenser, and immersed in an oil bath. In a typical experiment, *N*-phenylpropyl-3,4-dichlorobenzylsulfonamide (0.5 mmol), *s*-trioxane (1.5 mmol), and the appropriate amount of catalyst in toluene (2 mL) were heated to 70 °C with magnetic stirring (600 rpm) for 3 h. The catalyst was filtered and washed with toluene (3 × 0.5 mL). The organic solution was dried over anhydrous magnesium sulfate. The desiccant was filtered, and the solution was concentrated. The benzazepines (and related compounds) were recrystallized from acetone or ethyl acetate to afford the corresponding pure products.

3.4. Catalyst Reuse

The stability of PLMTPA60/40₁₀₀, the catalyst with the best performance, was evaluated in six consecutive runs, under identical reaction conditions. After each run, the catalyst was filtered from the reaction medium, washed with toluene, dried under vacuum, and then reused.

4. Conclusions

In the present work, we successfully modified the surface of the polymeric matrix by tungstophosphoric acid heterogeneous catalysts and characterized them by nitrogen adsorption–desorption isotherms, FT-IR, ³¹P MAS-NMR, DTA-TGA, SEM, XRD, and potentiometric titration. The catalysts were then used for the synthesis of *N*-(sulfonyl)-2,3,4,5-tetrahydro-1*H*-benzo[*c*]azepines and analogous rings. This methodology requires a short reaction time of 3 h and a temperature of 70 °C to obtain very good yields of benzo[*c*]azepines and analogous rings. An 83% yield was achieved in toluene and 1% PLMW60/40₁₀₀, the catalyst with the greater number of acid sites. The recyclability and reuse of the PLMW60/40₁₀₀ catalyst were established for up to six successive runs with no dramatic loss in the reaction profile.

Supplementary Materials: The following supporting information can be downloaded at: <https://www.mdpi.com/article/10.3390/catal12101155/s1>, include leaching analysis; characterization technique details; digital photograph; complementary FT-IR, potentiometric curves, and TGA of the catalysts; and the ¹H and ¹³C NMR spectra and melting points of synthesized benzazepines and related compounds. Figure S1: PLMTPA60/40₁₀₀ catalyst spheres; Figure S2: FT-IR spectrum of PLMTPA60/40 treated at 100 (PLMTPA40/60_{T100}), 200 (PLMTPA40/60_{T200}), and 300 °C (PLMTPA40/

60_{T300}); Figure S3: Potentiometric titration curves of PLMTPA60/40_{T100}, PLMTPA60/40_{T200}, and PLMTPA60/40_{T300} samples; Table S1: Weight loss of the polymer and catalysts obtained by TGA.

Author Contributions: Conceptualization, L.R.P. and G.P.R.; methodology, E.X.A.P., A.G.S., L.R.P. and G.P.R.; formal analysis, E.X.A.P., V.P., A.G.S., L.R.P. and G.P.R.; investigation, E.X.A.P. and V.P.; data curation, E.X.A.P., V.P., A.G.S. and L.R.P.; writing—review and editing, E.X.A.P., V.P., L.R.P. and G.P.R.; supervision, A.G.S., L.R.P. and G.P.R.; project administration, L.R.P. and G.P.R.; funding acquisition, L.R.P. and G.P.R.. All authors have read and agreed to the published version of the manuscript.

Funding: This work was supported by UNLP (A349, X879) and CONICET (PIP0111, PIP1492).

Data Availability Statement: Not applicable.

Acknowledgments: The authors thank the microscopy and analytical departments of CINDECA for the experimental measurement.

Conflicts of Interest: The authors declare no conflict of interest.

References

- Anastas, P.T.; Heine, L.G.; Williamson, T.C. Chapters 1–6. In *Green Chemical Syntheses and Processes*; Anastas, P.T., Heine, L.G., Williamson, T.C., Eds.; American Chemical Society: Washington, DC, USA, 2000.
- Hazarika, P.; Gogoi, P.; Hatibaruah, S.; Konwar, D. A green synthesis of 3,4-dihydropyrimidin-2-ones and 1,5-benzodiazepines catalyzed by Sn(HPO₄)₂·H₂O nanodisks under solvent-free condition at room temperature. *Green Chem. Lett. Rev.* **2011**, *4*, 327–339. [\[CrossRef\]](#)
- Suprita; Singh, R.; Suman; Susheel. Green methods for synthesis of various Heterocycles: Sustainable approach. *Int. J. Chem. Stud.* **2017**, *5*, 479–485.
- Sharma, S.; Gangal, S.; Rauf, A. Green chemistry approach to the sustainable advancement to the synthesis of heterocyclic chemistry. *Rasayan J. Chem.* **2008**, *1*, 693–717.
- Arico, F.; Reiser, O. Green synthesis of heterocycles. In *Frontiers*; Frontiers Media: SA, USA, 2020. [\[CrossRef\]](#)
- Morales, D.M.; Frenzel, R.A.; Romanelli, G.P.; Pizzio, L.R. Synthesis and characterization of nanoparticulate silica with organized multimodal porous structure impregnated with 12-phosphotungstic acid for its use in heterogeneous catalysis. *Mol. Catal.* **2020**, *481*, 110210. [\[CrossRef\]](#)
- Trombettoni, V.; Franco, A.; Sathicq, A.G.; Len, C.; Romanelli, G.P.; Vaccaro, L.; Luque, R. Efficient liquid-assisted grinding selective aqueous oxidation of sulfides using supported heteropolyacid catalysts. *ChemCatChem* **2019**, *11*, 1–10. [\[CrossRef\]](#)
- Escobar, A.; Blanco, M.; Martínez, J.; Cubillos, J.; Romanelli, G.; Pizzio, L. Biomass derivative valorization using nano core-shell magnetic materials based on Keggin-heteropolyacids: Levulinic acid esterification kinetic study with n-butanol. *J. Nanomater.* **2019**, *2019*, 5710708. [\[CrossRef\]](#)
- Patel, A. *Environmentally Benign Catalysts for Clean Organic Reactions*; Springer: Berlin/Heidelberg, Germany, 2013.
- Monopoli, V.D.; Pizzio, L.R.; Blanco, M.N. Polyvinyl alcohol–polyethyleneglycol blends with tungstophosphoric acid addition: Synthesis and characterization. *Mater. Chem. Phys.* **2008**, *108*, 331–336. [\[CrossRef\]](#)
- Fuchs, V.M.; Pizzio, L.R.; Blanco, M.N. Synthesis and characterization of aluminum or copper tungstophosphate and tungstosilicate immobilized in a polymeric blend. *Eur. Polym. J.* **2008**, *44*, 801–807. [\[CrossRef\]](#)
- Frenzel, R.; Morales, D.; Romanelli, G.; Sathicq, G.; Blanco, M.; Pizzio, L. Synthesis, characterization and catalytic evaluation of H3PW12O40 included in acrylic acid/acrylamide polymer for the selective oxidation of sulfides. *J. Mol. Catal. A Chem.* **2016**, *420*, 124–133. [\[CrossRef\]](#)
- Fuchs, V.M.; Pizzio, L.R.; Blanco, M.N. Hybrid materials based on aluminum tungstophosphate or tungstosilicate as catalysts in anisole acylation. *Catal. Today* **2008**, *133–135*, 181–186. [\[CrossRef\]](#)
- Frenzel, R.A.; Romanelli, G.P.; Pizzio, L.R. Novel catalyst based on mono- and di-vanadium substituted Keggin polyoxometalate incorporated in poly(acrylic acid-co-acrylamide) polymer for the oxidation of sulfides. *Mol. Catal.* **2018**, *457*, 8–16. [\[CrossRef\]](#)
- Frenzel, R.A.; Palermo, V.; Sathicq, A.G.; Elsharif, A.M.; Luque, R.; Pizzio, L.R.; Romanelli, G.P. A green and reusable catalytic system based on silicopolyoxotungstovanadates incorporated in a polymeric material for the selective oxidation of sulfides to sulfones. *Micropor. Mesopor. Mater.* **2021**, *310*, 110584. [\[CrossRef\]](#)
- Shah, J.H.; Hindupur, R.M.; Pati, H.N. Pharmacological and biological activities of benzazepines: An overview. *Curr. Bioact. Compd.* **2015**, *11*, 170–189. [\[CrossRef\]](#)
- Trybulski, E.J.; Benjamin, L.-E.; Earley, J.V.; Fryer, R.I.; Gilman, N.W.; Reeder, E.; Walser, A.; Davidson, A.B.; Horst, W.D.; Sepinwall, J.; et al. 2-Benzazepines. 5. Synthesis of pyrimido[5,4-d][2]benzazepines and their evaluation as anxiolytic agents. *J. Med. Chem.* **1983**, *26*, 1589–1596. [\[CrossRef\]](#)
- Gini, A.; Bamberger, J.; Luis-Barrera, J.; Zurro, M.; Mas-Ballesté, R.; Alemán, J.; García Mancheño, O. Synthesis of 3-benzazepines by metal-free oxidative C–H bond functionalization–ring expansion tandem reaction. *Adv. Synth. Catal.* **2016**, *358*, 4049–4056. [\[CrossRef\]](#)

19. Damsen, H.; Niggemann, M. Calcium-catalyzed synthesis of 1,2-disubstituted 3-benzazepines. *Eur. J. Org. Chem.* **2015**, *36*, 7880–7883. [\[CrossRef\]](#)
20. Dorgan, R.J.; Elliot, R.L. Benzazepines, and Their Use as Anthelmintics. U.S. Patent 4,661,489, 28 April 1987.
21. Abe, K.; Saitoh, T.; Horiguchi, Y.; Utsunomiya, I.; Taguchi, K. Synthesis and neurotoxicity of tetrahydroisoquinoline derivatives for studying Parkinson's disease. *Biol. Pharm. Bull.* **2005**, *28*, 1355–1362. [\[CrossRef\]](#)
22. Chuk, M.K.; Balis, F.M.; Fox, E. Trabectedin. *Oncologist* **2009**, *14*, 794–799. [\[CrossRef\]](#)
23. Iwasa, K.; Moriyasu, M.; Tachibana, Y.; Kim, H.S.; Wataya, Y.; Wiegrebe, W.; Bastow, K.F.; Cosentino, L.M.; Kozuka, M.; Lee, H.K. Simple isoquinoline and benzyloisoquinoline alkaloids as potential antimicrobial, antimalarial, cytotoxic, and anti-HIV agents. *Bioorg. Med. Chem.* **2001**, *9*, 2871–2884. [\[CrossRef\]](#)
24. Nandakumar, A.; Muralidharan, D.; Perumal, P.T. Synthesis of functionalized tetrahydroisoquinolines via palladium-catalyzed 6-*exo-dig* carbocyclization of 2-bromo-*N*-propargylbenzylamines. *Tetrahedron Lett.* **2011**, *52*, 1644–1648. [\[CrossRef\]](#)
25. So, M.; Kotake, T.; Matsuura, K.; Inui, M.; Kamimura, A. Concise synthesis of 2-benzazepine derivatives and their biological activity. *J. Org. Chem.* **2012**, *77*, 4017–4028. [\[CrossRef\]](#) [\[PubMed\]](#)
26. Elangovan, S.; Afanaserko, A.; Haupenthal, J.; Sun, Z.; Liu, Y.; Hirsch, A.K.H.; Barta, K. From wood to tetrahydro-2-benzazepines in three waste-free steps: Modular synthesis of biologically active lignin-derived scaffolds. *ACS Cent. Sci.* **2019**, *5*, 1707–1716. [\[CrossRef\]](#) [\[PubMed\]](#)
27. Szatmári, I.; Fülöp, F. Solvent-free synthesis of 1-(hydroxyquinolyl)- and 1-(hydroxyisoquinolyl)-1,2,3,4-tetrahydroisoquinolines by modified Mannich reaction. *Synthesis* **2011**, *5*, 745–748. [\[CrossRef\]](#)
28. Ruchirawat, S.; Tontoolarug, S.; Sahakitpichan, P. Synthesis of 4-aryltetrahydroiso-quinolines: Application to the synthesis of cherulline. *Heterocycles* **2001**, *55*, 635–640. [\[CrossRef\]](#)
29. Venugopal, S.; Ramanatham, J.; Devanna, N.; Sanjeev Kumar, A.; Ghosh, S.; Soundararajan, R.; Kale, B.; Mehta, G.N. New strategy for the synthesis of (±) cherylline dimethyl ether. *Asian J. Chem.* **2010**, *22*, 1835–1840.
30. Orazi, O.O.; Corral, R.A.; Giaccio, H. Synthesis of fused heterocycles: 1,2,3,4-tetrahydroisoquinolines and ring homologues *via* sulphonamidomethylation. *J. Chem. Soc. Perkin Trans. I* **1986**, 1977–1982. [\[CrossRef\]](#)
31. Pasquale, G.; Ruiz, D.; Autino, J.; Baronetti, G.; Thomas, H.; Romanelli, G. Efficient and suitable preparation of *N*-sulfonyl-1,2,3,4-tetrahydroisoquinolines and ring analogues using recyclable $H_6P_2W_{18}O_{62} \cdot 24H_2O/SiO_2$ catalyst. *C. R. Chim.* **2012**, *15*, 758–763. [\[CrossRef\]](#)
32. Romanelli, G.P.; Ruiz, D.M.; Autino, J.C.; Giaccio, H.E. A suitable preparation of *N*-sulfonyl-1,2,3,4-tetrahydroisoquinolines and their ring homologs with a reusable Preyssler heteropolyacid as catalyst. *Mol. Divers.* **2010**, *14*, 803–807. [\[CrossRef\]](#) [\[PubMed\]](#)
33. Pizzio, L.R.; Vázquez, P.; Kikot, A.; Basaldella, E.; Cáceres, C.; Blanco, M.N. Functionalized SiMCM-41 as support for heteropoly-acid based catalysts. *Stud. Surf. Sci. Catal.* **2002**, *143*, 739–746.
34. Hasik, M.; Turek, W.; Stochmal, E.; Lapkowski, L.; Pron, A. Conjugated polymer-supported catalysts-polyaniline protonated with 12-tungstophosphoric acid. *J. Catal.* **1994**, *147*, 544–551. [\[CrossRef\]](#)
35. Morales, M.D.; Infantes-Molina, A.; Lázaro-Martínez, J.M.; Romanelli, G.P.; Pizzio, L.R.; Rodríguez-Castellón, E. Heterogeneous acid catalysts prepared by immobilization of $H_3PW_{12}O_{40}$ on silica through impregnation and inclusion, applied to the synthesis of 3H-1,5-benzodiazepines. *Mol. Catal.* **2020**, *485*, 110842. [\[CrossRef\]](#)
36. Okuhara, T.; Nishimura, T.; Watanabe, H.; Na, K.; Misono, M. *Acid-Base Catalysis II*; Kodansha: Tokyo, Japan; Elsevier: Amsterdam, The Netherlands, 1994.
37. Massart, R.; Contant, R.; Fruchart, J.; Ciabrin, J.; Fournier, M. ^{31}P NMR studies on molybdic and tungstic heteropolyanions. Correlation between structure and chemical shift. *Inorg. Chem.* **1977**, *16*, 2916–2921. [\[CrossRef\]](#)
38. Pizzio, L.R.; Cáceres, C.V.; Blanco, M.N. Acid catalysts prepared by impregnation of tungstophosphoric acid solutions on different supports. *Appl. Catal. A Gen.* **1998**, *167*, 283–294. [\[CrossRef\]](#)
39. Fuchs, V.M.; Soto, E.L.; Blanco, M.N.; Pizzio, L.R. Direct modification with tungstophosphoric acid of mesoporous titania synthesized by urea-templated sol-gel reactions. *J. Colloid Interface Sci.* **2008**, *327*, 403–411. [\[CrossRef\]](#) [\[PubMed\]](#)
40. Silva, M.E.S.R.e.; Dutra, E.R.; Mano, V.; Machado, J.C. Preparation and thermal study of polymers derived from acrylamide. *Polym. Degrad. Stab.* **2000**, *67*, 491–495. [\[CrossRef\]](#)
41. Grassie, N.; McNeill, I.C.; Samson, J.N.R. The thermal degradation of polymethacrylamide and copolymers of methacrylamide and methyl methacrylate. *Eur. Polym. J.* **1978**, *14*, 931–937. [\[CrossRef\]](#)
42. Gorsd, M.; Pizzio, L.; Blanco, M. Trifluoromethanesulfonic acid immobilized on zirconium oxide obtained by the sol-gel method as catalyst in paraben synthesis. *Appl. Catal. A Gen.* **2011**, *400*, 91–98. [\[CrossRef\]](#)
43. Pizzio, L.R.; Cáceres, C.V.; Blanco, M.N. Tungstophosphoric acid immobilized in polyvinyl alcohol hydrogel beads as heterogeneous catalyst. *Stud. Surf. Sci. Catal.* **2002**, *143*, 731–738.
44. Pizzio, L.R.; Blanco, M.N. Isoamyl acetate production catalyzed by $H_3PW_{12}O_{40}$ on their partially substituted Cs or K salts. *Appl. Catal. A Gen.* **2003**, *255*, 265–277. [\[CrossRef\]](#)
45. Trost, B. The Atom Economy—A Search for Synthetic Efficiency. *Science* **1991**, *254*, 1471–1477. [\[CrossRef\]](#)
46. Anastas, P.T.; Warner, J.C. *Green Chemistry: Theory and Practice*; Oxford University Press: New York, NY, USA, 1998.
47. Andraos, J. Unification of reaction metrics for Green Chemistry: Applications to reaction analysis. *Org. Process. Res. Dev.* **2005**, *9*, 149–163. [\[CrossRef\]](#)

-
48. Andraos, J. Useful tools for the next quarter century of Green Chemistry practice: A dictionary of terms and a data set of parameters for high value industrial commodity chemicals. *ACS Sustain. Chem. Eng.* **2018**, *6*, 3206–3214. [[CrossRef](#)]
 49. Andraos, J. *The Algebra of Organic Synthesis*; CRC Press: Boca Raton, FL, USA, 2019.
 50. Kano, S.; Yuasa, Y.; Shibuya, S. Formation of alcohols from alkenes by reaction with $\text{SnCl}_4\text{--NaBH}_4$. *J. Chem. Soc. Chem. Commun.* **1979**, *18*, 796–797. [[CrossRef](#)]